Influence of oxygen addition to the carrier gas on Laser-Induced Breakdown Spectroscopy measurements on aerosols

N. Palazzo, F. Migliorini, R. Dondè, S. Maffi, S. De Iuliis*

CNR-IENI, Istituto per l'Energetica e le Interfasi

*Corresponding author

Silvana De Iuliis

IENI-CNR, Istituto per l'Energetica e le Interfasi

via Cozzi 53, 20125 Milano, Italy

deiuliis@ieni.cnr.it

Phone: +39-02-66173297

Fax: +39-02-66173321

Abstract

In this work laser-induced breakdown spectrosopy is implemented on aerosol particles for absolute concentration analysis. Aim of this work is the investigation of the effect of the bath gas used for nebulizing the aerosol. Nitrogen, air and 50% O_2 in N_2 mixture have been chosen as carrier gases in order to analyze the effect of oxygen addition to the gas. LIBS measurements have been carried out on aerosol particles produced from $CuCl_2$ $2H_2O$ solutions, and the 324.7 nm Cu line is considered. As a first analysis, plasma parameters, such as temperature and electron density, have been evaluated changing the carrier gas. Measurements to derive the LIBS calibration curve of the 324.7 nm Cu line are carried out in air and in N_2. The significant difference in the slope of the resulting calibration curves has to be attributed to the oxygen addition to the bath gas. To explore such behavior, time-resolved measurements of the Cu line and peak/base ratio have been performed. The presence of two competitive effects have been observed that becomes significant increasing the amount of oxygen in the carrier gas. One is the oxygen quenching effect, already observed in the literature, and the other one is the enhancement of the Cu LIBS signal, expecially at short delay times. These effects have been observed also at other Cu lines and changing the analyte source. The results are presented and widely discussed.

Keywords: Laser-Induced Breakdown Spectroscopy, Spectrochemical analysis, Cu analyte, carrier gas interference

1. Introduction

The analysis of aerosol particles is currently of great interest in different research areas due to the wide range of applications. Monitoring of combustion processes and their effluent waste streams, the analysis and characterization of particulate air pollution and engineered nanoparticles are only some of these applications. Several aerosol measurement techniques have been devised encompassing a broad range of operating principles. Most of these diagnostics, however, being essentially based on ex-situ analysis are time-consuming and require a proper sampling preparation. Atomic absorption spectroscopy (AAS), inductively coupled plasma optical emission spectroscopy (ICP-OES), or mass spectrometry (ICP-MS) essentially involve collecting sample for subsequent analysis [1-3]. Hence, due also to the particular applications, there is a need to promote the development and application of suitable on-line and / or time-resolved analytical techniques. A powerful and challenging analytical technique well suited for on-line *elemental* analysis of aerosols is laser-induced breakdown spectroscopy (LIBS). This is an atomic emission spectroscopy technique that utilizes a laser-induced microplasma which functions as both the sample volume and the excitation source [4-5]. A pulsed laser beam is tightly focused in a particle source flow. The resulting optical breakdown decomposes and excites all species within the plasma volume. The light emission is characterized by a continuum spectrum containing discrete atomic lines. These lines, both neutral (I) and ionic (II), and the continuum emission decay with time, but persist strongly on the order of tens of microseconds. In general the continuum spectrum decay faster than the atomic lines allowing the possibility of detecting atomic lines with a good signal-to-noise ratio by adjusting the delay and the integration time of the detector gate. However from an analytical point of view all the quantitative aspects of LIBS are still under study to better understand the complex nature of the laser-sample and plasma-particle interaction processes which depend on the laser pulse characteristics, sample properties, space and time [6-7]. Applications of the LIBS technique cover a wide range of species and compounds indicating that nearly all elements of interest in aerosol analysis are readily accessible with LIBS [8-10]. Several examples of the applicability of LIBS technique to investigate and measure elemental concentration of several analytes, e.g. metals, in ambient air are reported in the literature [11-14]. Size, mass and composition of micron and submicron aerosol particles have been evaluated [6], in most cases with the comparison and/or coupling with other techniques for aerosol characterization [12-13]. A lot of work has been done on LIBS signal processing, especially concerning the statistical analysis of single shots for detection of individual aerosol particle in dilute flow streams for atmospheric aerosol application. In this case, in fact, a proper conditional analysis has also been introduced [12, 14, 15], in order to take into account the non-uniform distribution of the analyte under investigation in the gas stream and consequently in the probe volume. As for quantitative analysis,

the application of LIBS is far to be trivial. Many parameters have to be taken into account, including plasma homogeneity issues, particle size limits and gas matrix effects [16]. Concerning the effect of the carrier gas used to generate the aerosol on LIBS signal, to our knowledge only few works can be found in the literature. Aerosols are usually produced with purified air, however sometimes the use of purified N_2 could be interesting. In the work of Gleason et al. [17], the mercury atomic emission produced via breakdown has been considered and the effect of the presence of oxygen species investigated. It has been observed that the mercury emission line is selectively quenched by oxygen species, primarily O_2 and NO, formed by atoms recombination during the plasma decay. This result produces also strong effects on LIBS signal calibration. In the work of Buckley [18], different analytes have been investigated with the aim to look at the effect on the LIBS signal using N_2 or air to produce the aerosol. For Pb and Be a reduction in the slope of the calibration curve passing from N_2 to air has been obtained due to oxygen quenching in agreement with the Hg behavior reported by Gleason et al. [17]. On the contrary, a different behavior has been exhibited by Cr. The influence of the bath gas on the LIBS signal has also been explored in the work of Pieler et al. [19] where aluminum metal measurements have been carried out.

In this work the investigation of the influence of the carrier gas on LIBS signals is performed on aerosol particles of copper. Copper was chosen as representative analyte for environmental monitoring purpose because it can be released into the environmental air by both natural sources (wind-blown dust, decaying vegetation, forest fires, rocks weathering and sea spray) and human activities (mining, electrical factories, metal production, construction, transportation, and phosphate fertilizer production) [20-21]. The aerosol has been produced by using alternatively purified N_2, purified air and 50% O_2 in N_2 mixture to nebulize and dilute/dry the aerosol droplets. In order to characterize the plasma, temperature and electron density have been evaluated. The calibration curves of 324.7 nm Cu LIBS signal have been obtained in air and N_2. In order to explore the different slope of the resulting calibration curves, time-resolved 324.7 nm Cu LIBS measurements have been carried out in the presence of the carrier gases under analysis. Same behavior has been obtained also for other Cu lines and changing the analyte source. The detected differences have been discussed relatively to the chemical and thermal effects due to oxygen addition.

2. LIBS measurements

2.1 Experimental Set-up

In Fig. 1 the experimental apparatus employed for LIBS measurements is shown. A pulsed Nd:YAG laser (Continuum, 7 ns FWHM) at the fundamental wavelength (1064 nm), with 5 Hz repetition rate

and 220 mJ pulse energy was used to produce the plasma by means of a 80-mm focal length lens. The plasma spectral emission was collected perpendicularly to the incident laser beam by means of two plano-convex lenses (focal length = 100 mm and 75 mm) onto an optical fiber (3 mm diameter) coupled with the detection unit. The latter consists of a Czerny-Turner spectrograph (Shamrock 303i) equipped with a turret of three gratings, and coupled with an intensified charge coupled device ICCD (iStar 321T, Andor Technology) camera. For these measurements, the high resolution grating (1200 grooves/mm) resulting in 0.113 nm resolution was used. The intensified CCD detector was synchronized with the Q-switch laser in order to change the delay and the integration width of the detector gate.

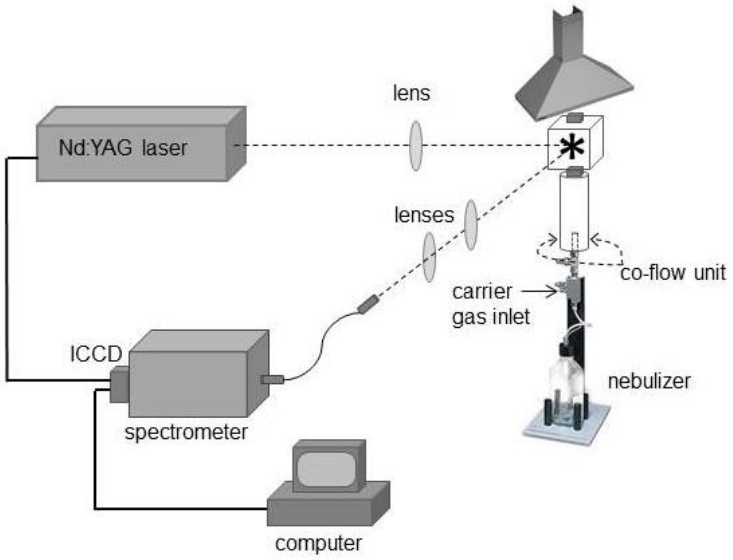

Fig. 1 Experimental set-up.

LIBS measurements were performed directly in the aerosol sample chamber, that is a stainless steel six ways chamber properly equipped with optical windows. Aerosol particles were produced from nebulized solutions of $CuCl_2\,2H_2O$ in ultra-purified deionized water. The particle source stream was generated using a constant output atomizer (TSI model 3075), which allows us to obtain fine droplets of about 300 nm. The droplets stream was introduced into a mixing/drying section. Here the uniform carrier co-flow gas flowing around the nebulizer output permitted to facilitate droplets vaporization via mass diffusion of water to the surrounding gas and to produce a fine dispersion of metallic salt. The resulting dried particles in the aerosol stream were carried by the co-flow gaseous stream into the sample chamber.

Knowing the droplet dimension, the solution concentration and the salt density, the size of the dried particles was calculated to range between 14 and 30 nm. Uniform aerosol with a reasonable number

of nanometric particles in the probe volume was used in order to perform reliable and robust calibration curves.

For a nebulization flow rate of 3 lpm and a co-flow of 17.5 lpm, the aerosol particle number density in the sample chamber was approximately $4.6*10^8$ particles per cubic centimeter. In this case such a high number density of nanometric particles provided a uniform aerosol. Moreover, while the laser spot is $4.6*10^{-8}$ cm^3, the measured plasma volume results to be 0.5 mm^3, according to the work of Carranza et al. [22]. Correspondingly, a number of particle of $2*10^5$ was present, which is representative of an average concentration in the sample chamber. Consequently each laser shot produced a LIBS analyte signal. Each LIBS spectrum was collected as an ensemble-average of 500 multiple spectra, without applying any conditional analysis. In fact, it has been verified by collecting separately 500 LIBS spectra that each laser shot heats the analyte and consequently each spectrum exhibited the corresponding LIBS signal.

For both LIBS calibration curves and LIBS signal behavior versus delay time the most sensitive emission line of neutral Cu at 324.7 nm was considered.

3. Results and discussion

3.1 Plasma characterization

In order to evaluate the influence of oxygen addition, plasma was investigated by using three different carrier gases (N_2, air and 50% O_2 in N_2 mixture). In our condition the plasma can be considered in local thermodynamic equilibrium (LTE) [23, 24], which means that the emission from a particular atomic or ionic line is related to the elemental concentration, the electron density and the temperature. The population density of atomic and ionic electronic states can be described by a Boltzmann distribution. As a first analysis the temperature and electron density were investigated for the different carrier gases.

Plasma temperature was calculated from the slope of the Einstein-Boltzmann equation. Considering a transition taking place between an upper level *m* to a lower level *n*, the Einsten-Boltzmann equation can be written as

$$ln\frac{\lambda_{mn}I_{mn}}{g_m A_{mn}} = ln\left(\frac{N(T)}{U(T)}\right) - \frac{E_m}{k_b T} \quad (1)$$

where λ_{mn} is the wavelength of the transition, I_{mn} is the atomic line intensity, A_{mn} is the transition probability, E_m is the energy of the upper level, g_m is the statistical weight of level *m*, k_b is the

Boltzmann constant and T is the excitation temperature. By plotting $ln\frac{\lambda_{mn}I_{mn}}{g_m A_{mn}}$ versus E_m, temperature can be obtained from the slope of the curve, without knowing the total number density *N(T)* or the partition function *U(T).*

In our case for temperature measurement three nitrogen neutral lines, namely 410.99 nm, 821.63 nm and 746.8 nm, were used. In Table 1 the spectroscopic parameters used to evaluate plasma temperature are reported, as taken from the National Institute of Standards and Technology (NIST) [25].

Electron density was calculated from the stark broadened profile of the nitrogen line at 746.83 nm. The full width at half maximum [FWHM] of the spectral line is expressed as [26-27]

$$\Delta\lambda_{1/2} = 2\omega\frac{\mathrm{N_e}}{10^{16}} \quad (2)$$

where N_e is the electron density (in cm^{-3}) and ω is the electron impact parameter, obtained from reference data [28]. Temperature and electron density measurements were performed at 5, 10 and 15 μs delay time and a fixed gate width of 10 μs and the corresponding results are reported in Table 2. In particular, in the table temperature uncertainties are also shown for the different conditions under analysis. As one can observe in the table, there is no significant difference among plasma parameters in the three carrier gases under analysis, even considering the temperature uncertainty of 16% in the worst case (at 5 μs delay). These results indicate that thermal effects of oxygen addition to the carrier gas can be considered negligible.

3.2 Calibration curves

LIBS signal intensity was evaluated using the area of the 324.7 nm atomic peak divided by a representative baseline area. This last quantity has been calculated by taking the trapezoid area at the base of the LIBS atomic line. Assuming an optically thin plasma, the atomic emission line area is proportional to the elemental concentration and depends on the laser power, while the baseline is proportional to the laser power. Consequently the peak/baseline area ratio, referred as peak/base in the following, is proportional to the elemental concentration only. At concentrations below approximately 50 mg/m^3 self-absorption can be considered negligible and the calibration curves using the peak/base ratio are generally linear [18].

Calibration curves were performed in purified nitrogen and air by analyzing dry $CuCl_2$ aerosols. Once the aqueous solution concentration, nebulization rate, flow rate and co-flow gases rate are known, the

analyte concentration in the aerosol stream at the LIBS sample point can be easily determined as reported by Gleason et al. [17]

$$X = \frac{(Neb.Rate)\,(Sol.concentration)}{(Co{-}flow\ Rate{+}Neb.flow\ Rate)} \quad (3)$$

In Fig. 2 high resolution LIBS spectra, corresponding to a 8.25 mg/m^3 Cu concentration, are reported as obtained for N_2, air and 50% O_2 in N_2 mixture plasma. The signals have been collected with a gate width of 10 μs and a delay time of 20 μs. The two typical Cu atomic lines at 324.7 and 327.39 nm, whose intensities surprisingly increase by adding oxygen to the mixture, are shown. No significant difference in the baseline can be detected close to the 324.7 nm Cu peak, consistently with no change in the electron density by varying the carrier gas. An increase in the baseline in correspondence of Cu at 327.39 nm is observed for N_2 and air which is due to the presence of N_2^+ bands at 329.4 nm and 329.9 nm.

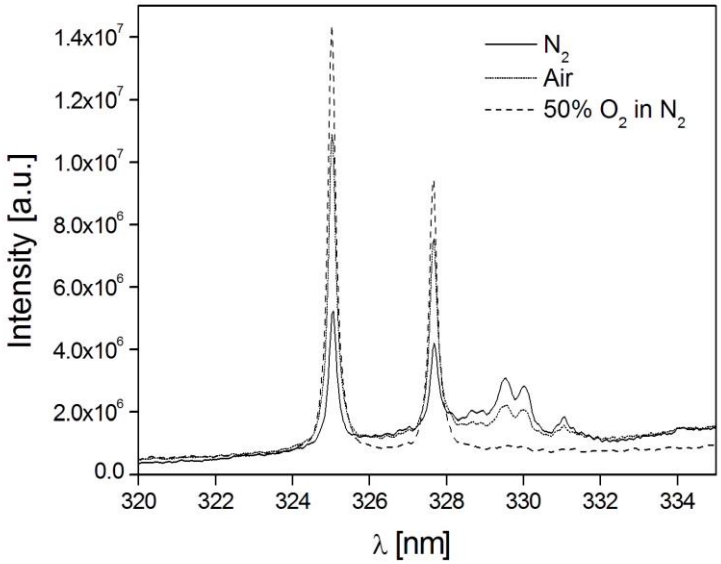

Fig. 2 LIBS intensity versus wavelength for the carrier gases. Spectra are collected with a gate width of 10 μs and a delay of 20 μs.

In the present study, for Cu calibration curve, the values of copper mass concentration in the flow stream range from 0.82 mg/m^3 to 6 mg/m^3. Spectra were collected at 30 μs delay time, with respect to the plasma-initiating laser pulse, and a fixed integration time of 100 μs.

Cu calibration curves in nitrogen compared with the calibration curve in air are reported in Fig. 3. In this case the calibration in 50% O_2 in N_2 mixture was not performed, being of no analytical interest. In the same figure the linear fitting and the related analytical expressions as well as the error bars for each LIBS peak/base measurements are reported. As for signal/base uncertainties, a value of 5% for the standard deviation is obtained in the worst case. The values of the determination coefficient R^2 account for a good linear relationship between the LIBS intensity and the particle mass concentration. Although both signal responses are linear with respect to the concentration of Cu, a different slope of the calibration curves have been obtained using nitrogen and air as carrier gas. Surprisingly, at a given Cu concentration higher values of LIBS signals are obtained in the case of air with respect to nitrogen as carrier gas in contrast to the quenching effect of O_2 observed in [17] for Hg.

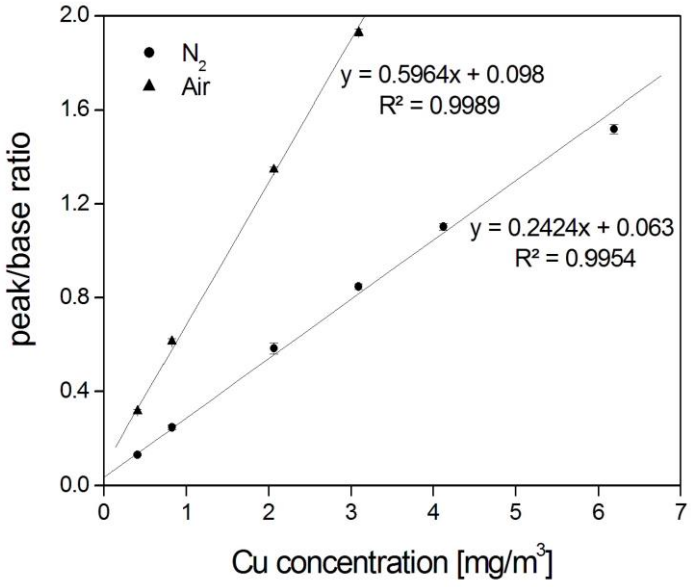

Fig. 3 Calibration curves of Cu in nitrogen and air, and the corresponding linear regression. Peak/base ratio are reported with the related error bars.

Different values of the detection limit are derived in the two cases. According to Cremers et al. [29], the lower limit of detection, LOD, defined as the lowest quantity of a substance that can be distinguished from the background within a stated confidence limit (1%) is given by

$$LOD = \frac{3\sigma_B}{S} \quad (4)$$

where σ_B is the standard deviation of the background and S is the slope of the calibration curve. Considering the standard deviation as calculated from the background intensity values for each mass concentration, the LOD of Cu signal was 66 μg/m^3 in air , while 117 μg/m^3 in nitrogen. In this context

the difference in the two cases are put in evidence rather than the relatively high value of the detection limit, which is not the purpose of this work.

3.3 LIBS signal as a function of delay time

In order to investigate the influence of the carrier gas on the calibration curve, the temporal behavior of the Cu emission signal was performed changing the carrier gas. To this purpose, measurements were carried out with N_2, air (20% O_2 in N_2) and 50% O_2 in N_2 mixture. LIBS signals were collected varying the delay and using gate widths of 1 μs and 10 μs at short and long delay time, respectively. In fact, after 50 μs delay time the Cu LIBS signal is too low to be detected and therefore to increase the signal/noise ratio, the gate width was increased to 10 μs. In Figs. 4 and 5 the integrals of 324.7 nm Cu LIBS peak and the corresponding peak/base signals are reported versus delay time for N_2, air and 50% O_2 in N_2 mixture. Close and open symbols refer to measurements collected with 1 μs and 10 μs gate widths, respectively.

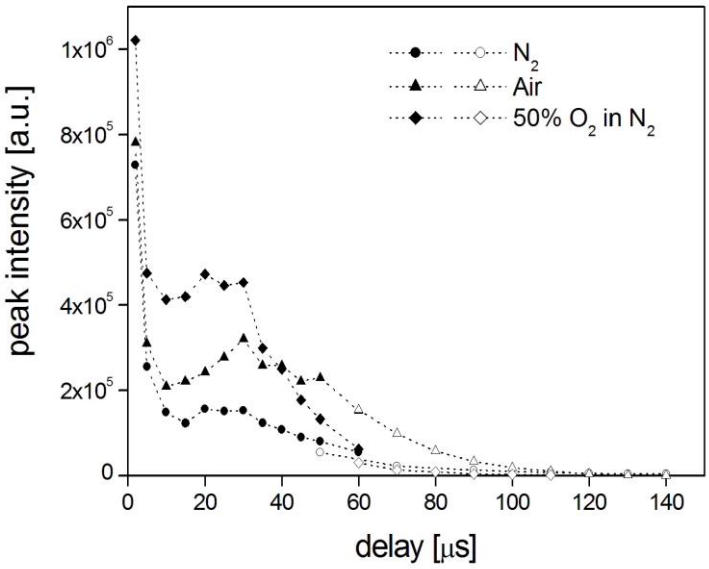

Fig. 4 Cu LIBS peak value versus delay time in N_2, air and 50% O_2 in N_2 mixture. $CuCl_2$ $2H_2O$ is the analyte source.

Measurements with 10 μs gate width have been properly corrected for the different gate width. Same behavior of the two curves is obtained also for the 327.39 nm atomic line and is not reported here for brevity. As for the LIBS signal (Fig. 4), in all the investigated conditions the overall curve exhibits a behavior widely different from the usual exponential decay trend. In particular, LIBS signal decreases almost exponentially up to 10 μs, after which an anomalous increase of the signal is detected followed

by a further exponential decrease. Comparing the curves obtained with different carrier gas, it is evident that at short delay time LIBS signal increases by increasing O_2 percentage in the mixture. Moreover, at longer delay time, e.g. 60 μs, LIBS signal increases passing from N_2 to air, and then decreases for 50% O_2 in N_2 mixture. The small bump in the LIBS signal detected after 10 μs in the case of N_2 can also be due to the presence of oxygen both in the solution and in the analyte source.

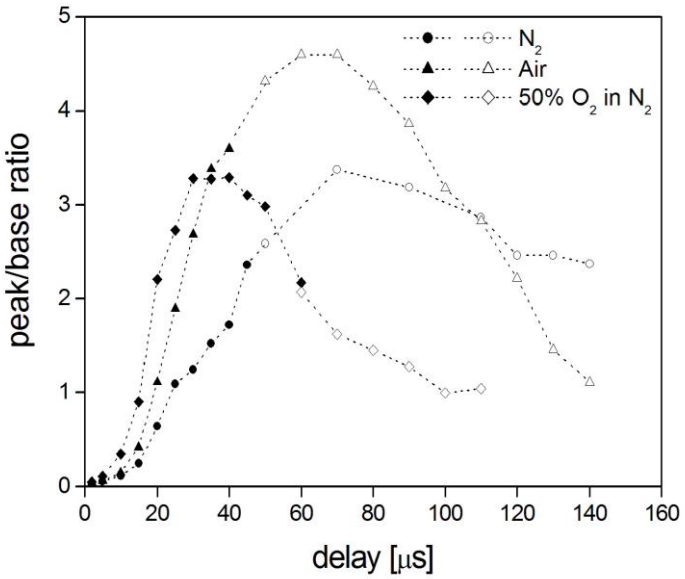

Fig. 5 Cu LIBS peak/base value versus delay time in N_2, air and 50% O_2 in N_2 mixture. $CuCl_2$ $2H_2O$ is the analyte source.

As for peak/base behavior (Fig. 5) changing the carrier gas a significant difference in the Cu peak/base curves is observed. Moving from N_2 to air the curve increases and becomes narrower. A further increase of O_2 percentage results in a peak/base value decrease and shift toward shorter delay times. In order to better understand the effect of O_2 addition to the carrier gas, the ratio of the peak/base curves of air or 50% O_2 in N_2 mixture to the N_2 curve (all reported in Fig. 5) was considered and shown in Fig. 6.

As it can be seen, the effect of O_2 addition is different along all the time scale investigated. In fact, at short delay times an enhancement of the LIBS signal is observed, while at longer delay O_2 is responsible for signal quenching. In the case of air/N_2 curve the transition between the two competitive effects (enhancement and quenching) occurs in a wider temporal scale producing a smooth behavior of the overall trend. Moreover, the effect of adding O_2 to the carrier gas up to 50% is to further increase the enhancement (about twice the amount) and at the same time to shorten the transition time between the two competitive effects. From Fig. 6 it is evident that by using air as

carrier gas the LIBS signal enhancement due to oxygen is more effective than the quenching effect at least for the delay and gate width used.

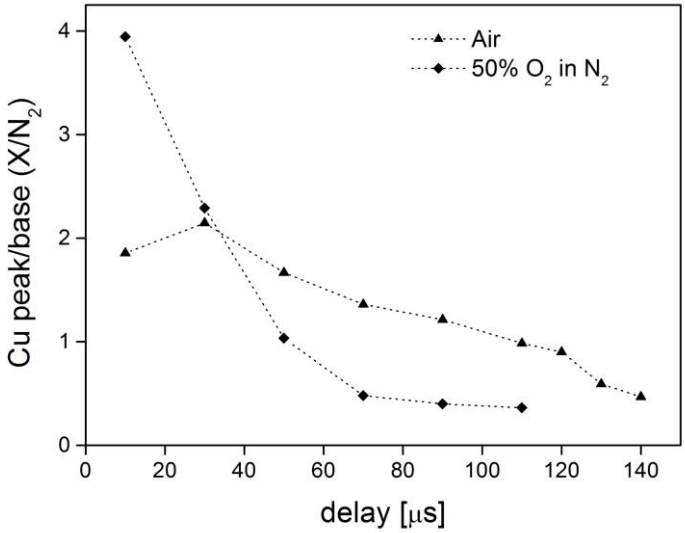

Fig. 6 Ratio of Cu peak/base curves of air and 50% O_2 in N_2 mixture with respect to N_2 peak/base curve.

While the quenching effect of O_2 addition has been already observed [17] and reported in different papers, to our knowledge very few evidence concerning LIBS signal enhancement effect are present in the literature. In the work of Buckley[18] different atomic species have been investigated in relation to the role of O_2 addition to the carrier gas. In the case of Pb and Be O_2 quenching is evident and responsible for a reduction of LIBS signal passing from N_2 to air. On the contrary, a small increase in the Cr LIBS emission intensity has been observed comparing N_2 and air. Unfortunately no hypothesis has been proposed to explain the process at the basis of such effect. Moreover, concerning O_2 quenching, it is also observed that such effect relevant to a given analyte atomic line is not observed in other transition of the same analyte [17]. For this reason also the Cu lines at 510.5 nm, 515.3 nm and 521.8 nm have been investigated. These Cu LIBS lines detected at different delay times exhibit the same behavior as the one obtained for 324.7 nm (Figs. 4, 5), and are not here reported.
Actually the enhancement of Cu LIBS signal in presence of air can be due to thermal or/and kinetics effects. The substantial unchanged values of temperature and electron density of the plasma in different bath gases (see Table 1) allow us to infer that no thermal effect is possible. On the contrary some kind of kinetic pathway could play an important role in this process. Moreover, it is also evident that molecular or/and atomic oxygen has to be involved in these reactions. To further investigate the role of oxygen, the time behavior of O(I) LIBS signal at 777 nm has also been detected and compared

to the corresponding Cu LIBS signal. As an example, in Fig. 7 the trend obtained in air is reported. As it can be seen, the atomic oxygen intensity decreases significantly already in the first 10 μs. Correspondingly, the unusual increase of Cu emission intensity after 10 μs could be due to an energy transfer process which involves the Cu line.

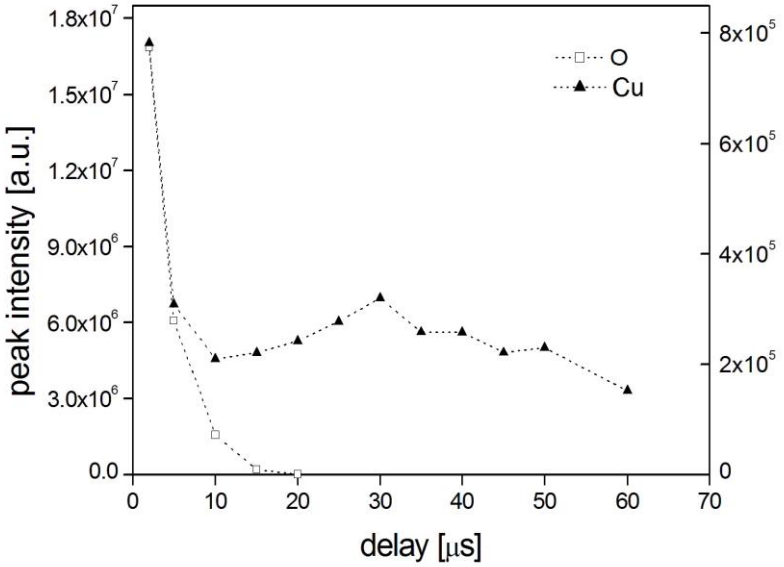

Fig. 7 Comparison of LIBS signal of O(I) at 777 nm and Cu(I) at 324 nm versus delay time in air.

One possible explanation could be the formation of a molecular oxygenated species in its excited level, which in turn could be resonant with Cu 324.7 nm emission line. Unfortunately no molecular species emit in this spectral region, and however this process would not explain the same behavior at 327.39 nm.

Also the presence of Cl in the analyte source can play a role in the kinetic mechanisms responsible for the enhancement of the Cu LIBS signal. It is well known that both Cl atomic line and molecular emission involving Cl can be detected only at relatively high concentration (e.g. 50 ppm) in the work of Haisch et al. [30] due to low sensitivity. In fact in our case, no evidence of Cl atomic or molecular emission is observed at least in the spectral region under analysis.

Therefore, in order to investigate a possible role of the analyte source, $CuCl_2\ 2H_2O$ has been replaced by $CuSO_4\ 12H_2O$. In Fig. 8 LIBS signal of Cu at 324.7 nm versus delay time have been reported for the three carrier gases under analysis. Varying the carrier gas, the temporal curves exhibit the same trend as the one obtained with $CuCl_2\ 2H_2O$ as analyte source (see Fig. 4).

These observations allow us to infer that the Cl does not contribute to the Cu LIBS signal enhancement.

Another explanation could be a three body collisional recombination involving two oxygen atoms and a sample atom, Cu in our case. This reaction results in sample atom excitation by the molecular recombination energy.

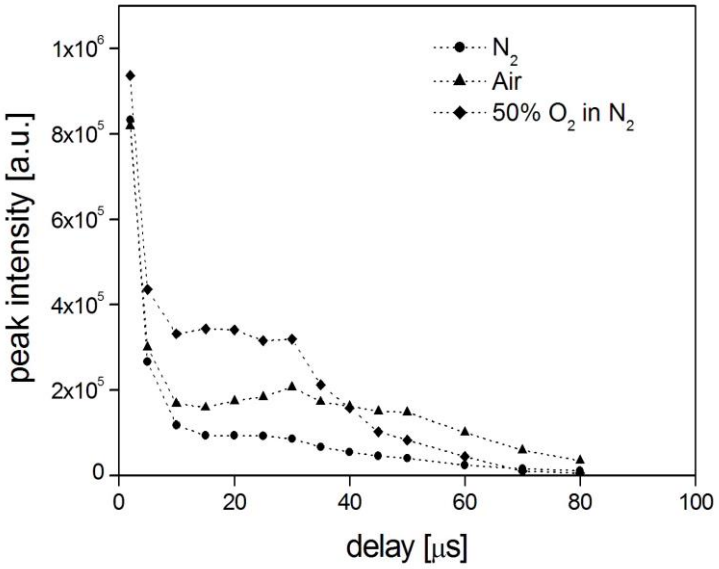

Fig. 8 Cu LIBS peak value versus delay time in N_2, air and 50% O_2 in N_2 mixture. $CuSO_4\,12H_2O$ is the analyte source.

This process has been proposed by Mushtaq et al. [31] to explain the enhancement of analyte atomic line in glow discharges. As energy O_2 recombination is 5 eV [31] analyte atomic lines with excitation energy near to this value can be enhanced. This is not our case, as the excitation energy of the Cu line 324.7 nm is about 3.8 eV. However, due to the different experimental conditions of the discharges as well as the amount of O_2 added to the bath gas (usually less than 1% in the work of Mushtaq et al. [31] and 20% in our case) one can speculate about the occurrence of the three body recombination involving oxygen in other excited levels. More work is needed to address such issue.

5. Conclusions

In this work the influence of the presence of O_2 in the carrier gas on LIBS measurements performed on aerosol particles of copper is investigated. To this purpose, $CuCl_2\,2H_20$ is used as analyte source and the 324.7 nm Cu LIBS signal has been considered for this analysis. Nitrogen, air and 50% O_2 in N_2 mixture have been chosen as nebulizing gas. Plasma temperature and electron density have been measured in the different conditions under analysis. Calibration curves as well as the behavior of Cu

peak line and peak/base ratio versus delay time have been investigated changing the carrier gas. The results are reported in the following.

- No substantial differences have been observed on plasma temperature and electron density measured. This means that no thermal effect in the plasma is produced changing the gas.
- As for Cu calibration curves, a significant increase of the curve slope is detected changing N_2 with air in the bath gas.
- The temporal behavior of Cu LIBS signal exhibits a decay trend very far from the usual exponential one, with an anomalous bump after about 10 μs decay time.
- In both the LIBS peak and peak/base measurements, two competitive phenomena are observed: an enhancement of the LIBS signal more significant at short delay time and a signal quenching at long delay time. Both effects are more important with increasing the oxygen amount in the carrier gas.
- The behavior obtained for 324.7 nm Cu line is also exhibited by the 327.39 nm as well as 510.5 nm, 515.3 nm and 521.8 nm Cu lines. Same results have also been obtained changing the Cu analyte source.
- Atomic oxygen (at 777 nm) decreases fast in the first 10 μs, which could account for molecular oxygen formation.

According to this observation, it is possible to infer that the signal quenching is essentially due to the presence of molecular oxygen, in agreement with previous results reported in the literature. As for the signal enhancement, such effect can be certainly attributed to the presence of oxygen. One possible hypothesis could be the occurrence of the three body recombination involving oxygen in some excited levels. More work is needed to address such issue. In any case, it is important to stress that care has to be taken in performing the calibration curve of an analyte when using O_2 in the carrier gas.

Acknowledgment

The authors acknowledge the financial support provided by INTEGRATE project in the framework of CNR-Regione Lombardia program. The authors wish to thank Mr. E. Fantin for his technical support.

Figure Captions

Fig. 1: Experimental set-up.

Fig. 2: LIBS intensity versus wavelength for the carrier gases. Spectra are collected with a gate width of 10 μs and a delay of 20 μs.

Fig. 3: Calibration curves of Cu in nitrogen and air, and the corresponding linear regression. Peak/base ratio are reported with the related error bars.

Fig. 4: Cu LIBS peak value versus delay time in N_2, air and 50% O_2 in N_2 mixture. $CuCl_2$ $2H_2O$ is the analyte source.

Fig. 5: Cu LIBS peak/base value versus delay time in N_2, air and 50% O_2 in N_2 mixture. $CuCl_2$ $2H_2O$ is the analyte source.

Fig. 6: Ratio of Cu peak/base curves of air and 50% O_2 in N_2 mixture with respect to N_2 peak/base curve.

Fig. 7: Comparison of LIBS signal of O(I) at 777 nm and Cu(I) at 324 nm versus delay time in air.

Fig. 8: Cu LIBS peak value versus delay time in N_2, air and 50% O_2 in N_2 mixture. $CuSO_4$ $12H_2O$ is the analyte source.

Table Captions

Table 1. Transition probability-statistical weight product, lower and upper energy levels for N(I) emission lines used in this work.

Table 2. Plasma temperature and electron density as a function of delay time for air, N_2 and 50% O_2 in N_2 mixture.

References

[1] A. F. Lagalante, Atomic Absorption Spectroscopy: a tutorial review, Appl. Spectrosc. Rev. 34 (3) (2004) 173–189.

[2] S. Ghosh, V. L. Prasanna, B. Sowjanya, P. Srivani, M. Alagaraja, Dr. D. Banji, Inductively Coupled Plasma – Optical Emission Spectroscopy: a review, Asian J. Pharm. Ana. 3(1) (2013) 24-33.

[3] D. Profrock, A. Prange, Inductively Coupled Plasma – Mass Spectrometry (ICP-MS) for quantitative analysis in environmental and life sciences: a review of challenges, solutions, and trends, Appl. Spectrosc. 66(8) (2012) 843-868.

[4] D. W. Hahn, Laser-Induced Breakdown Spectroscopy for analysis of aerosol particles: the path toward quantitative analysis, Spectroscopy 24(9) (2009) 26-33.

[5] P. K. Diwakar, P. Kulkarni, Laser-Induced Breakdown Spectroscopy for analysis of aerosols, in: S. Musazzi and U. Perini (Eds.) Laser-Induced Breakdown Spectroscopy, Springer Series in Optical Sciences, Springer-Verlag Berlin Heideberg, 2014, 227-255.

[6] D. W. Hahn, Laser-Induced Breakdown Spectroscopy for sizing and elemental analysis of discrete aerosol particles, Appl. Phys. Lett. 72 (1998) 2960-2962.

[7] A. Molina, C. R. Shaddix, S. M. Sickafoose, P. M. Walsh, L. G. Blevins, Effect of temperature and CO_2 concentration on Laser-Induced Breakdown Spectroscopy measurements of alkali fume, Spectrochim. Acta B 60 (2005) 1103-1114.

[8] R. E. Neuhauser, U. Panne, R. Niessner, Laser-Induced Plasma Spectroscopy (LIPS): a versatile tool for monitoring heavy metal aerosols, Anal. Chim. Acta 392 (1999) 47-54.

[9] U. Panne, R. E. Neuhauser, M. Theisen, H. Fink, R. Niessner, Analysis of heavy metal aerosols on filters by Laser-Induced Plasma Spectroscopy, Spectrochim. Acta B 56 (2001) 839-850.

[10] K. Park, G. Cho, and J. Kwak, Development of an aerosol focusing Laser-Induced Breakdown Spectroscopy (Aerosol Focusing-LIBS) for determination of fine and ultrafine metal aerosols, Aerosol Sci. Tech. 43 (2009) 375–386.

[11] G. A. Lithgow, A. L. Robinson, S. G. Buckley, Ambient measurements of metal-containing PM2.5 in an urban environment using Laser-Induced Breakdown Spectroscopy, Atmos. Environ. 38 (2004) 3319-3328.

[12] G. Gallou, J. B. Sirven, C. Dutouquet, O. Le Bihan, E. Frejafon, Aerosol analysis by LIBS for monitoring of air pollution by industrial sources, Aerosol Sci. Tech. 45 (2011) 918-926.

462 [13] D. W. Hahn, J. E. Carranza, G. R. Arsenault, H. A. Johnsen, K. R. Hencken, Aerosol generation
463 system for development and calibration of laser-induced breakdown spectroscopy instrumentation,
464 Rev. Sci. Instrum. 72 (2001) 3706-3713.
465 [14] J. E. Carranza, B. T. Fisher, G. D. Yoder, D. W. Hahn, On-line analysis of ambient air aerosols
466 using Laser-Induced Breakdown Spectroscopy, Spectrochim. Acta B 56 (2001) 851-864.
467 [15] D. Hahn, W. L. Flower, K. R. Hencken, Discrete particle detection and metal emissions
468 monitoring using Laser-Induced Breakdown Spectroscopy, Appl. Spectrosc. 51(12) (1997) 1836-
469 1844.
470 [16] V. Hohreiter and D. W. Hahn, Calibration effects for Laser-Induced Breakdown Spectroscopy
471 of gaseous sample streams: analyte response of gas-phase species versus solid phase species, Anal.
472 Chem. 77 (2005) 1118-1124.
473 [17] R. L. Gleason, D. W. Hahn, The effects of oxygen on the detection of mercury using Laser-
474 Induced Breakdown Spectroscopy, Spectrochim. Acta B 56 (2001) 419-430.
475 [18] S. G. Buckley, Laser-Induced Breakdown Spectroscopy for toxic metal emission measurements:
476 experimental considerations and oxygen quenching, Environ. Eng. Sci. 22 (2005) 195-203.
477 [19] T. N. Piehler, F. C. DeLucia, C. A. Munson, B. E. Homan, A. W. Miziolek, K. L. McNesby,
478 Temporal evolution of the laser-induced breakdown spectroscopy spectrum of aluminium metal in
479 different bath gases, Appl. Optics 44(18) (2005) 3654-3660.
480 [20] J. M. Pacyna, Atmospheric trace elements from natural and anthropogenic sources. In: J. O.
481 Nriagu, and C. I. Davidson, eds., Toxic metals in the atmosphere. Advances in Environmental Science
482 and Technology. John Wiley & Sons. Inc., 1986.
483 [21] P. M. Nirel, F. Pasquini, Differentiation of copper pollution origin: agricultural and urban
484 sources, Novatech 2010: International conference on sustainable techniques and strategies in urban
485 water management, Lyon 27 June -1 July 2010.
486 [22] J. E. Carranza, D. W. Hahn, Plasma volume considerations for analysis of gaseous and aerosol
487 samples using laser-induced breakdown spectroscopy, J. Anal. Atom. Spectrom. 17 (2002) 1534-
488 1539.
489 [23] S. Yalcin, D. R. Crosley, G. P. Smith, G. W. Faris, Influence of ambient conditions on the laser
490 air spark, Appl. Phys. B 68 (1999) 121-130.
491 [24] G. Cristoforetti, A. De Giacomo, M. Dell'Aglio, S. Legnaioli, E. Tognoni, V. Palleschi, N.
492 Omenetto, Local Thermodynamic Equilibrium in Laser-Induced Breakdown Spectrosocpy: Beyond
493 the MsWhirter criterion, Spectrochim. Acta B 65 (2010) 86-95.
494 [25] National Institute of Standards and Technology (NIST) electronic database, available at:
495 http://physics.nist.gov/PhysRefData/ASD/lines_form.html.

[26] N. M. Shaikh, B. Rashid, S. Hafeez, Y. Jamil and M. A. Baig, Measurement of electron density and temperature of a laser-induced zinc plasma, J. Phys. D: Appl. Phys. 39 (2006) 1384–1391.

[27] P. Stavropoulos, A. Michalakou, G. Skevis, S. Courisa, Laser-Induced Breakdown Spectroscopy as an analytical tool for equivalence ratio measurement in methane–air premixed flames, Spectrochim. Acta B 60 (2005) 1092 – 1097.

[28] H. R. Griem, Plasma Spectroscopy, McGraw Hill, New York, 1964.

[29] D. A. Cremers, L. J. Radzuemski, Handbook of Laser-Induced Breakdown Spectroscopy, 2014 John Wiley & Sons, Ltd, 2014.

[30] C. Haisch, R. Niessner, O. I. Matveev, U. Panne, N. Omenetto, Element-specific determination of chlorine in gases by Laser-Induced Breakdown Spectroscopy (LIBS), J. Anal. Chem. 356 (1996) 21-26.

[31] S. Mushtag, E. B. M. Steers, J. C. Pickering and P. Smid, Enhancement of analyte atomic lines with excitation energies of about 5 eV in the presence of molecular gases in analytical glow discharge, J. Anal. Atom. Spectrom. 29 (2014) 2022-2026.